

## NUMERICAL INVESTIGATION INTO THE PERFORMANCE PEMFC WITH A WAVE-LIKE GAS FLOW CHANNEL DESIGN

Shiuh-Ming Chang \*, Jenn-Kun Kuo \*\*

\*Department of Mechanical and Automation Engineering  
Kao Yuan University  
Kaohsiung, 821, Taiwan  
\*\*Institute of Greenergy  
National University of Tainan  
Tainan 700, Taiwan

\*Corresponding author. Tel.:+886-7-6077028; Fax: +886-7-6077112  
E-mail address: [esmoo@cc.kyu.edu.tw](mailto:esmoo@cc.kyu.edu.tw)

### ABSTRACT

This paper investigates the performance of a proton exchange membrane fuel cell (PEMFC) with a novel wave-like gas flow channel. Numerical simulations are performed to investigate the effect of the wave-like channel profile on the gas flow characteristics, temperature distribution, electrochemical reaction efficiency, and electrical performance. The simulation results show that compared to a conventional straight gas flow channel, the wave-like channel increases the fuel flow velocity, enhances the transport through the porous layer, and improves the temperature distribution. As a result, the PEMFC has an improved fuel utilization efficiency and superior heat transfer characteristics. Furthermore, the results show that the wave-like gas flow channel yields a higher PEMFC output voltage and improves the maximum power density by approximately 32.5%.

### KEY WORDS

PEMFC; Numerical simulations; Wave-like gas flow channel

### 1. Introduction

Proton exchange membrane fuel cells (PEMFCs) are regarded as a viable power source for a variety of applications. The requirements for compactness, high power density, high performance, good electrical stability, and low cost have led to the optimization of many aspects of a PEMFC. Several PEMFC models have been presented in recent years. Bernardi and Verbrugge [1, 2] and Springer [3] proposed one-dimensional models which provide a good preliminary foundation for more advanced PEMFC modeling. The two-dimensional models presented by Nguyen and White [4] assumed that oxygen transport was driven by diffusion alone and neglected the effects of the gas diffusion layer (GDL) [5] and the gas flow field. Hence, the practical applicability of the model was somewhat limited. Recent years have seen a significant increase in the power densities, reliability and

electrical performance of fuel cells. However, the underlying physics of the transport mechanism in a fuel cell, which involves coupled fluid flow, heat and mass transfer and electrochemical reaction, remain poorly understood. Accordingly, researchers have increasingly adopted the use of computational fluid dynamics (CFD) simulations to model PEMFCs in order to obtain deeper insights into their transport mechanisms and performance characteristics.

A variety of PEMFC gas flow channel configurations have been proposed, including serpentine channels, multiple parallel channels, interdigitated channels, and so forth. The GDL forms one sidewall of the fuel channel in a PEMFC, and hence its morphology affects the transport of the reactant gas from the channel to the catalyst surface and must be taken into account. Conventional PEMFCs have straight gas flow channels. However, Kuo and Chen [6, 7] proposed the use of gas flow channels with a novel wave-like form to improve the PEMFC performance. Their results showed that the unique channel design improved the uniformity of the velocity and temperature distributions within the channel and reduced the included angle between the dimensionless velocity vector and the temperature gradient thereby improving the heat transfer characteristics of the fuel cell.

The current study presents a detailed numerical investigation into the velocity, temperature and gas concentration distributions within the wave-like gas flow channel. Additionally, the study compares the electrical performance of a PEMFC with wave-like gas flow channels with that of a PEMFC with conventional straight gas flow channels.

### 2. PEMFC model

The simulations performed in this study are based on a steady state, single-phase, multi-species, two-dimensional mass transfer model of a PEMFC. Figure 1 presents a 3D solid-rendered schematic illustration of the fuel cell. As shown, the fuel cell comprises anode and cathode flow channels with wave-like profiles, two gas diffusion layers

made of a porous material (carbon paper), two catalyst layers, and a proton exchange membrane. The geometric and physical parameters employed in the present simulations are summarized in Table 1 [3, 8]. Note that some minor parameters are omitted from this table, but can be found in the literature [9, 10]. The operating pressure and temperature are 1 atm and 323 K, respectively. The simulations assume that the anode is supplied with humidified hydrogen with a mass fraction of 70/30 % H<sub>2</sub>/H<sub>2</sub>O. The cathode side is fed with saturated air with a mass fraction of 21/79 % O<sub>2</sub>/N<sub>2</sub>. The N<sub>2</sub> gas is considered to be inert and serves as a diluent. An assumption is made that the hydrogen reactant gas enters the gas flow channel normal to the channel cross-section. The following additional assumptions are also made:

1. The gas mixture is an incompressible, ideal fluid.
2. The Reynolds number of the fluid is less than 200 and the flow is laminar.
3. The gas diffusion layer, the catalyst layer and the membrane are all isotropic and homogeneous, and are characterized by high permeability and a uniform porosity.
4. The electrochemical reaction is governed by Butler-Volmer kinetics.
5. The water byproduct of the electrochemical reaction at the cathode side is in a vapor state.
6. The membrane is impervious to the reactant gases.
7. The fuel cell geometry is periodic in the x-axis direction.

The governing equations are identical for both the wave-like channel and the conventional straight channel. In developing the model of the wave-like channel, it is assumed that the fuel cell geometry is periodic in the x-direction. Figure 2 shows the computational model constructed for the wave-like channel. For computational efficiency, the computational domain is divided into seven separate layers, namely the upper wave-like channel, the anode GDL, the anode catalyst layer (CL), the membrane, the cathode CL, the cathode GDL and the lower wave-like channel.

PEMFCs with various gas flow channel configurations have been presented in the literature. In general, the aim of all of these different pathways is to maximize the area of the reaction surface exposed to the oxygen and hydrogen gas streams and to provide a route for the liquid water produced during the catalytic reaction to exit the fuel cell. The wave-like gas flow channel considered in this study has the additional function of enhancing the gas velocity in the vertical direction in order to improve the efficiency of the catalytic process.

The heat and mass transfer in both a wave-like gas flow channel and a conventional straight gas flow channel can be modeled using conventional mass conservation, Navier-Stokes, and energy and species conservation equations [11].

The basic gas transport equations for a general 2D PEMFC are as follows:

Continuity equation:

$$\frac{\partial u}{\partial x} + \frac{\partial v}{\partial y} = 0 \quad (1)$$

Momentum equation:

$$\varepsilon_{eff} \left( u \frac{\partial u}{\partial x} + v \frac{\partial u}{\partial y} \right) = -\frac{\varepsilon_{eff}}{\rho} \frac{\partial P}{\partial x} + \nu \varepsilon_{eff} \left( \frac{\partial^2 u}{\partial x^2} + \frac{\partial^2 u}{\partial y^2} \right) + S_u \quad (2)$$

$$\varepsilon_{eff} \left( u \frac{\partial v}{\partial x} + v \frac{\partial v}{\partial y} \right) = -\frac{\varepsilon_{eff}}{\rho} \frac{\partial P}{\partial y} + \nu \varepsilon_{eff} \left( \frac{\partial^2 v}{\partial x^2} + \frac{\partial^2 v}{\partial y^2} \right) + S_v \quad (3)$$

Energy equation:

$$\varepsilon_{eff} C_p \left( u \frac{\partial T}{\partial x} + v \frac{\partial T}{\partial y} \right) = \frac{k \varepsilon_{eff}}{\rho} \left( \frac{\partial^2 T}{\partial x^2} + \frac{\partial^2 T}{\partial y^2} \right) + S_e \quad (4)$$

Species conservation equation:

$$\varepsilon_{eff} \left( u \frac{\partial C_k}{\partial x} + v \frac{\partial C_k}{\partial y} \right) = D_{k,eff} \left( \frac{\partial^2 C_k}{\partial x^2} + \frac{\partial^2 C_k}{\partial y^2} \right) + S_c \quad (5)$$

Charge conservation equation:

$$\varepsilon_{eff} \left( u \frac{\partial \phi_e}{\partial x} + v \frac{\partial \phi_e}{\partial y} \right) = -S_\phi \quad (6)$$

Table 2 presents the analytical formulae for the source terms  $S_u$ ,  $S_v$ ,  $S_e$ ,  $S_c$  and  $S_\phi$  in Eqs. (2) ~ (6). In these formulae, the parameters  $\varepsilon_{eff}$ ,  $C_F$ ,  $k_p$  and  $Z_f$  denote the effective porosity, the quadratic drag factor, the permeability and the valence of the species, respectively. Furthermore,  $D_{k,eff} = D_k \varepsilon^{\tau_i}$  represents the effective diffusion coefficient of the kth component of the reactant fuel [12].

In the PEMFC, the generation/consumption of the chemical species and the charge transfer are restricted to the catalyst layer. Therefore, the source terms in Eqs. (5) and (6) can be implemented based on electrochemical kinetics, i.e.

$$S_{H_2} = -\frac{j_{anode}}{2F} \quad (7)$$

$$S_{O_2} = -\frac{j_{cathode}}{4F} \quad (8)$$

$$S_{H_2O} = -\frac{j_{cathode}}{2F} \quad (9)$$

where  $j$  denotes the transfer current density and is derived from the following Butler-Volmer kinetics expressions:

$$j_a = j_{a,ref} \left( \frac{C_{H_2}}{C_{H_2,REF}} \right)^{1/2} \times \left[ \exp\left( \frac{\alpha_a F}{RT} \eta_{act} \right) - \exp\left( -\frac{\alpha_c}{RT} F \eta_{act} \right) \right] \quad (10)$$

$$j_c = -j_{a,ref} \left( \frac{C_{O_2}}{C_{O_2,REF}} \right) \times \left[ \exp\left( \frac{\alpha_a F}{RT} \eta_{act} \right) - \exp\left( -\frac{\alpha_c}{RT} F \eta_{act} \right) \right] \quad (11)$$

where  $\eta_{act}$  is the surface over potential and is defined as:

$$\eta_{act} = \varphi_{a,c} - \varphi_m - V_{OC} \quad (12)$$

in which  $\varphi_{a,c}$  and  $\varphi_m$  denote the potentials of the carbon phase and the membrane phase, respectively, in the catalyst layer, and  $V_{OC}$  is the reference open-circuit potential of the electrode.

The phase potential equation for the potential and current profile is given by:

$$\frac{\partial}{\partial x} \left( \sigma_m \frac{\partial \Phi}{\partial x} \right) + \frac{\partial}{\partial y} \left( \sigma_m \frac{\partial \Phi}{\partial y} \right) = S_j \quad (13)$$

where  $\Phi$  is the phase potential function and  $\sigma_m$  is the membrane conductivity, which has the form [3]:

$$\sigma_m(T) = \sigma_m^{ref} \exp \left[ 1268 \left( \frac{1}{303} - \frac{1}{T} \right) \right] \quad (14)$$

where  $\sigma_{m,ref}$  is the reference conductivity of the membrane and is given by:

$$\sigma_m^{ref} = 0.005139\lambda - 0.00326 \quad (15)$$

$$\lambda = \begin{cases} 0.043 + 17.81 \cdot a - 39.85 \cdot a^2 + 36.0 \cdot a^3 & \text{for } 0 < a \leq 1 \\ 14 + 1.4 \cdot (a - 1) & \text{for } 1 \leq a \leq 3 \end{cases} \quad (16)$$

in which  $a$  is the water activity and is defined as:

$$a = \frac{x_{H_2O} P}{P_{sat}} \quad (17)$$

In Eq. (17), the saturation pressure varies with the temperature and can be determined directly from thermodynamic tables or from the following empirical expression:

$$P_{sat} = 10^{-2.1794 + 0.02953T - 9.1837 \times 10^{-5} T^2 + 1.4454 \times 10^{-7} T^3} \quad (18)$$

### 3. Boundary conditions

The governing equations for the current PEMFC model are elliptic, partial differential equations, and hence boundary conditions are required for all of the boundaries in the computational domain. Due to the conjugated nature of the current problem, the gas flow channel surfaces are included within the solution domain and are treated as a particular type of fluid.

The boundary conditions are as follows:

1. Gas flow channel:

Anode inlet:

$$u = u_{in}, T = T_{in}$$

$$v = 0, C_{H_2} = C_{H_2,in}^a, C_{H_2O} = C_{H_2O,in}^a, \quad (19)$$

Cathode inlet:

$$u = u_{in}, T = T_{in}$$

$$v = 0, C_{O_2} = C_{O_2,in}^c, C_{N_2} = C_{N_2,in}^c, \quad (20)$$

Interface between gas flow channel walls and catalyst layer.

$$u = v = \frac{\partial C_k}{\partial x} = 0 \quad (21)$$

2. Gas flow channel outlet:

$$\frac{\partial u}{\partial x} = \frac{\partial v}{\partial x} = \frac{\partial T}{\partial x} = 0 \quad (22)$$

3. Upper surface:

Anode gas channel:

$$u = v = 0 \quad (23)$$

$$T_{surface} = 298K \quad (24)$$

4. Lower surface:

Cathode gas channel:

$$u = v = 0 \quad (25)$$

$$T_{surface} = 298K \quad (26)$$

$$T_{in} > T_w \quad (27)$$

## 4. Results and discussion

### 4.1 Velocity field

The transport phenomena in the gas flow channel and GDL of a PEMFC have a fundamental effect on the fuel cell performance. The fluid flow in the wave-like gas flow channel has an axial flow velocity ( $u$ ) and a flow vector in the  $y$ -direction ( $v$ ). Figure 3(a) shows the vertical (i.e.  $y$ -direction) velocity profile in a conventional straight gas flow channel for laminar flow with a PEMFC operating potential of 0.6V, a cathode gas flow inlet velocity of 0.4 m/s and an anode gas flow inlet velocity of 0.2 m/s. Meanwhile, Figure 3(b) illustrates the vertical velocity profile in the wave-like flow channel under the same conditions. It is apparent that the periodic wave-like structure of the proposed gas flow channel increases the velocity of the flow in the vertical direction. Hence, the catalytic reaction in the catalyst layer is enhanced, and the performance of the PEMFC is correspondingly improved. Figure 4 shows the distributions of the axial flow velocity in the wave-like gas flow channel and the straight gas flow channel, respectively. The local maximum velocities are indicated in both cases. In general, it is seen that the fuel side (anode) has a lower velocity than the air side (cathode) since the fuel has a smaller stoichiometric coefficient. Furthermore, it is apparent that the velocity is higher in the wave-like channel than in the straight channel. The maximum velocity occurs in the region immediately above the crests of the profiled surface. The velocity in the wave-like channel is higher than that in the straight channel because the constricted channel area above each crest introduces a nozzle-type effect which accelerates the flow. In general, the pressure drop characteristics are unaffected by the flow direction. Figures 3 and 4 show that for a cathode gas flow inlet velocity of 0.4 m/s and an anode gas flow inlet velocity of 0.2 m/s, the maximum  $y$ -direction velocity in the wave-like channel is 0.289 m/s and the maximum  $x$ -direction velocity is 1.0756 m/s. Furthermore, the figures show that the wave-like form of the gas channel causes the axial velocity to reduce in the valley regions of the channel. Hence, the provision of fuel to the reaction

layer is increased. Figures 3 and 4 also show that the wave-like form flow channel induces a strong convection force along the reaction surface. This further increases the supply of the reactant gases to the catalyst layers and also improves the removal of the reaction byproducts from the PEMFC. Thus, the performance of the fuel cell is significantly improved, particularly at higher current densities.

#### 4.2 Concentration distribution

Figures 5 and 6 show the oxygen and hydrogen concentrations in the wave-like and straight gas flow channels. Note that in both figures, the cathode over potential is 0.6 V and the color-coded scale indicates the normalized concentration of the two gases. Figure 6 shows that the oxygen concentration in the wave-like channel reduces slightly along the axial direction. Furthermore, it is observed that the oxygen concentration varies significantly in the GDL region, particularly near the reaction surface. By contrast, in the straight gas flow channel, the oxygen concentration near the reaction surface is relatively uniform. The greater variation in the oxygen concentration in the wave-like gas channel is the result of the forced convection effect in the diffusion layer, which permits more oxygen to diffuse through the layer, thereby enhancing the chemical reaction. By contrast, the straight gas flow channel achieves only a limited oxygen and hydrogen transfer rate in the reaction surface region since transport is achieved by diffusion only.

Figure 7 shows the oxygen concentration distributions in the wave-like and straight form gas flow channels, respectively, for a cell voltage of 0.6 V. It is seen that the oxygen mole fraction decreases along the flow direction as a result of absorption in the catalyst layer. Furthermore, it is apparent that the oxygen consumption is higher in the wave-like channel than in the straight channel.

#### 4.3 Polarization curve

The polarization characteristics of a PEMFC provide a convenient means of evaluating the performance of fuel cells with different gas flow channel configurations. Figure 8 shows the polarization and power density curves of PEMFCs with wave-like and straight gas flow channels, respectively. It is seen that for an oxygen inlet velocity of  $0.4\text{ m/s}$  and a hydrogen inlet velocity of  $0.2\text{ m/s}$ , the PEMFC with a wave-like gas channel yields a higher cell voltage and power density. For an oxygen inlet velocity of  $0.1\text{ m/s}$  and a hydrogen inlet velocity of  $0.05\text{ m/s}$ , both PEMFCs have a relatively poorer performance. However, the electrical performance of the PEMFC with the wave-like gas flow channel is still better than that of the PEMFC with the conventional straight channel since the wave-like surface increases the supply of oxygen to the reaction layer. Figure 8 also shows that the power density of the PEMFC with the wave-like gas flow channel is approximately 32.5%

higher than that of the PEMFC with the straight channel. This result demonstrates that the wave-like surface of the flow channel changes the transport of the reactant gas to the catalyst layer surface from a diffusion mechanism to a convection mechanism resulting in a significantly improved electrical performance.

## 5. Conclusion

This study has developed a two-dimensional computational model to study the transport phenomena in PEMFCs with wave-like gas flow channels and conventional straight gas flow channels, respectively. The heat transfer performance and gas flow velocity characteristics of the two channel geometries have been examined. The results have shown that compared to the conventional gas flow channel, the wave-like channel provides a significantly improved convective heat transfer performance and a higher gas flow velocity, which in turn improves the efficiency of the catalytic reaction. Furthermore, compared with a PEMFC with conventional straight gas flow channels, the PEMFC with wave-like gas flow channels has improved current density and polarization characteristics.

## References

- [1] D.M. Bernardi, M.W. Verbrugge, *AIChE J.* 37 (1991) 1151.
- [2] D.M. Bernardi, M.W. Verbrugge, *J. Electrochem. Soc.* 139 (1992) 2477.
- [3] T.E. Springer, T.A. Zawodzinski, S. Gottesfeld, *J. Electrochem. Soc.* 136 (1991) 2334.
- [4] T.V. Nguyen, R.E. White, A. Water, *J. Electrochem. Soc.* 140 (1993) 2178.
- [5] H. Meng, C.Y. Wang, *J. Electrochem. Soc.* 151 (2004) A358.
- [6] J.K. Kuo, C.K. Chen, *J. Power Sources*, 162 (2006) 207.
- [7] J.K. Kuo, C.K. Chen, *J. Power Sources*, 162 (2006) 1122.
- [8] J.J. Hwang, C.H. Chao, W.Y. Ho, C.L. Chang, D.Y. Wang, *J. Power Sources*, 153 (2006) 130.
- [9] V. Gurau, H. Liu, S. Kakac, *AIChE, J.* 46 (1998) 2410.
- [10] S. Um, C.Y. Wang, K.S. Chen, *J. Electrochem. Soc.* 147 (2000) 4485.
- [11] Y. Wang, C.Y. Wang, *J. Electrochem. Soc.* 152 (2005) A445.
- [12] C.Y. Wang, *Chemical Reviews* 104 (2004) 4727.

Table 1  
Geometric and physical parameters in PEMFC model

Quantity	Value
Gas channel depth	0.5 mm
Gas channel width	0.5 mm
Gas channel length	100 mm
Gas diffusion layer thickness	0.3 mm
Catalyst thickness	0.05 mm
Membrane thickness	0.125 mm
Porosity of gas diffusion layer	0.4
Porosity of catalyst layer	0.28
Permeability of gas diffusion layer	$1.76 \times 10^{-11} m^2$
Permeability of catalyst layer	$1.76 \times 10^{-11} m^2$
Permeability of membrane layer	$1.18 \times 10^{-18} m^2$
Tortuosity of gas diffusion layer	1.5
Tortuosity of catalyst layer	1.5
Electronic conductivity of gas diffusion layer	53 S/m
Electronic conductivity of catalyst layer	53 S/m
Inlet temperature	323 K
Operation pressure	1 atm
Anode fuel	$H_2, H_2O$
Cathode fuel	$O_2, N_2$
Relative humidity of the anode	100 %
Buoyancy (gravity)	$-9.81 m/s$

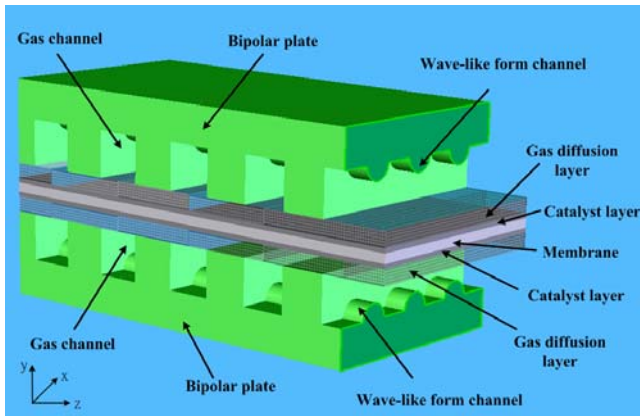


Figure 1. Schematic representation of PEMFC.

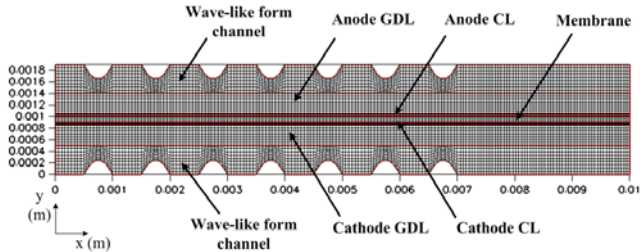
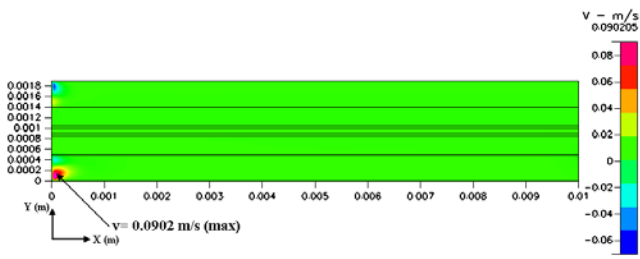


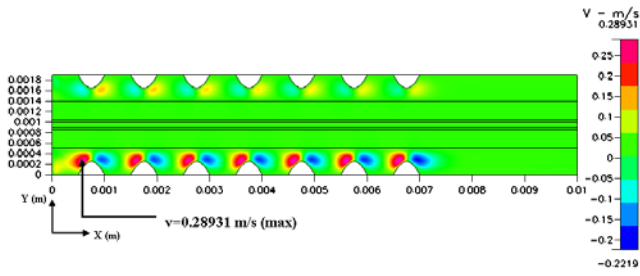
Figure 2. Computational domain of PEMFC gas flow channel.

Table 2 Analytical formulae for source terms in governing equations

	Membrane <sup>o</sup>	Catalyst Layer <sup>o</sup>	Gas Diffusion Layer <sup>o</sup>	Flow Channel <sup>o</sup>
$S_u^o$	$-\frac{v\varepsilon^2}{k_y}u - \frac{\varepsilon^2 C_F \rho u}{\sqrt{k_y}} \sqrt{ u ^2 + v^2} + \frac{k_y}{v} Z_f C_H + F \cdot \nabla \phi \frac{\partial u}{\partial x}$	$-\frac{v\varepsilon^2}{k_y}u - \frac{\varepsilon^2 C_F \rho u}{\sqrt{k_y}} \sqrt{ u ^2 + v^2}$	$-\frac{v\varepsilon^2}{k_y}u - \frac{\varepsilon^2 C_F \rho u}{\sqrt{k_y}} \sqrt{ u ^2 + v^2}$	$0^o$
$S_v^o$	$-\frac{v\varepsilon^2}{k_y}v - \frac{\varepsilon^2 C_F \rho v}{\sqrt{k_y}} \sqrt{ u ^2 + v^2} + \frac{k_y}{v} Z_f C_H + F \cdot \nabla \phi \frac{\partial v}{\partial x}$	$-\frac{v\varepsilon^2}{k_y}v - \frac{\varepsilon^2 C_F \rho v}{\sqrt{k_y}} \sqrt{ u ^2 + v^2}$	$-\frac{v\varepsilon^2}{k_y}v - \frac{\varepsilon^2 C_F \rho v}{\sqrt{k_y}} \sqrt{ u ^2 + v^2}$	$0^o$
$S_e^o$	$\frac{i_m^2}{\rho k_m}$	$\rho \left[  n_{an}  - \frac{T \Delta S}{nF} \right] + \rho \left( \frac{i_m^2}{k_m} + \frac{i_e^2}{k_y} \right)$	$\rho \frac{i_e^2}{k_y}$	$0^o$
$S_c^o$	$\frac{ZF}{RT} D_{k_{eff,H^+}} C_{H^+} \left( \frac{\partial^2 \phi}{\partial x^2} + \frac{\partial^2 \phi}{\partial y^2} \right)$	$H_2 : -\frac{j_a}{2FC_e} \quad O_2 : -\frac{j_c}{4FC_e}$	$H_2 : -\frac{j_a}{2FC_e} \quad O_2 : -\frac{j_c}{4FC_e}$	$0^o$
$S_\phi^o$	$0^o$	$j^o$	$0^o$	$0^o$

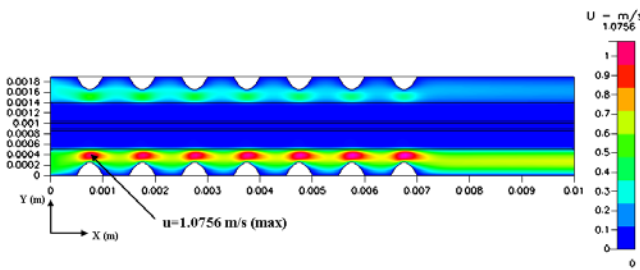


(a). Straight geometry.

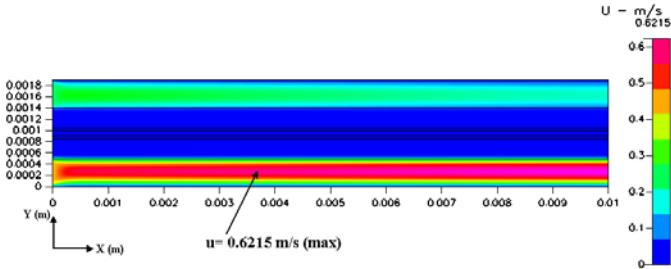


(b) Wave-like geometry.

Figure 3. Velocity field in y-direction of gas flow channels.

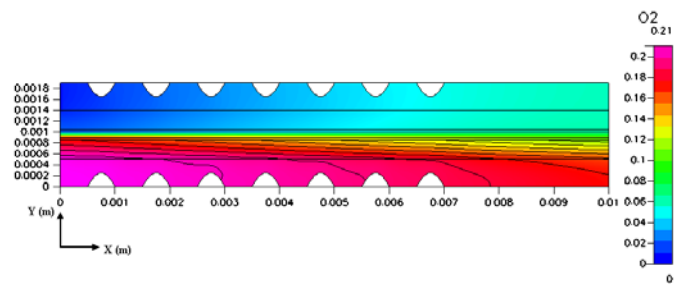


(a) Wave-like geometry.

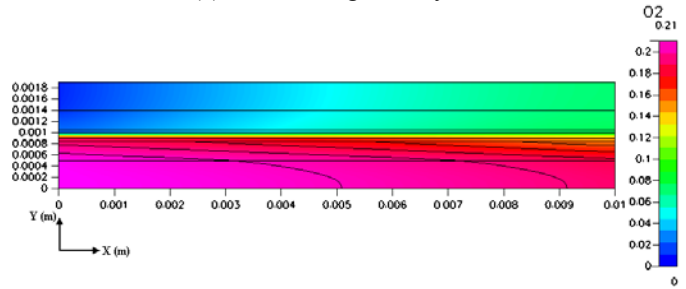


(b) Straight geometry.

Figure 4. Velocity field in x-direction of gas flow channels.

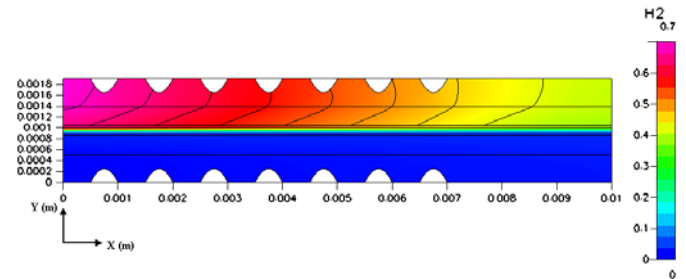


(a) Wave-like geometry.

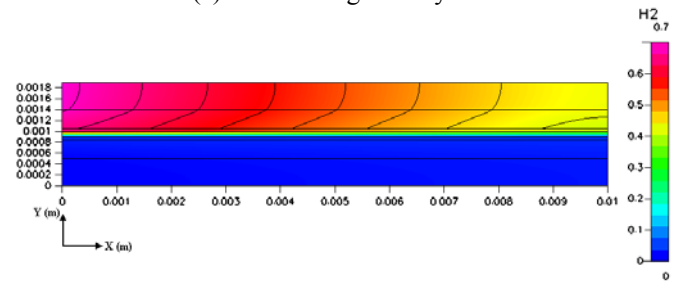


(b) Straight geometry.

Figure 5. Oxygen concentration distribution in gas flow channels at cell voltage of 0.6 V.



(a) Wave-like geometry.



(b) Straight geometry.

Figure 6. Hydrogen concentration distribution in gas flow channels at cell voltage of 0.6 V.

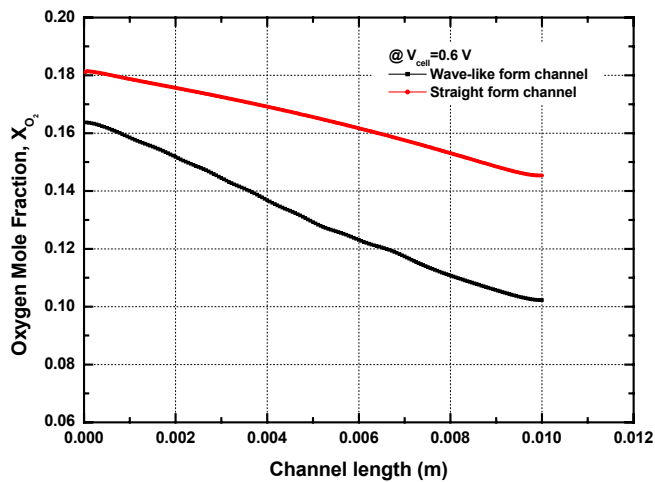


Figure 7. Oxygen mole fraction profiles in cathode catalyst layers of gas flow channels at cell voltage of 0.6V.

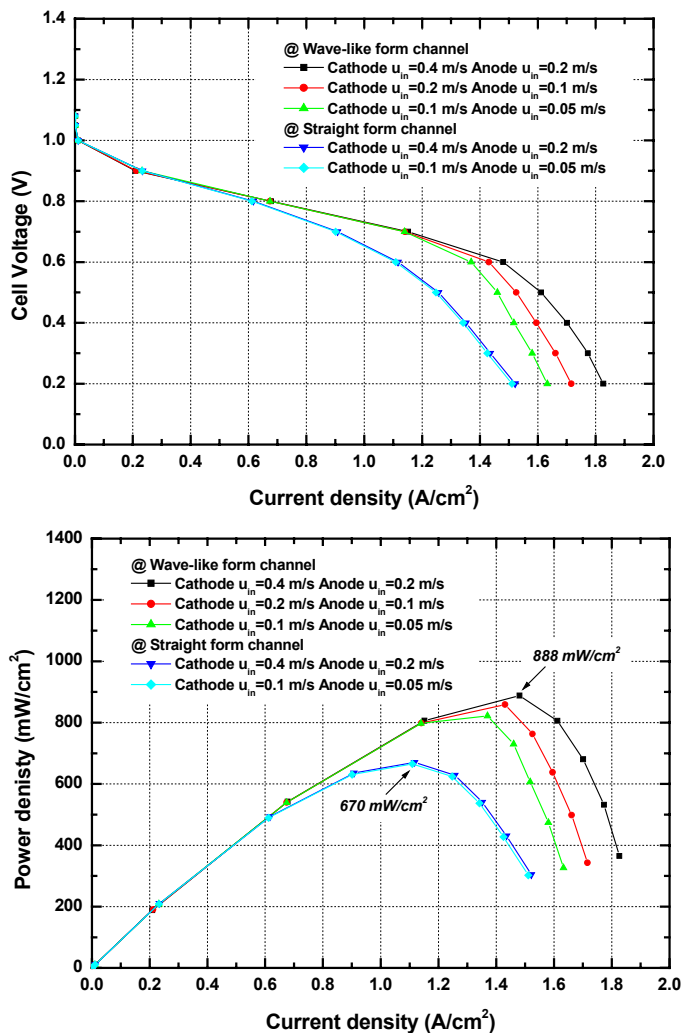


Figure 8. (a) Polarization curve and (b) power density curve in gas flow channels for various inlet velocity conditions.